

# Analysis of Recent Trends in Single Image Dehazing Techniques

Jenisha C, Sheeba Joice C

Saveetha Engineering College, Saveetha Nagar, Thandalam, Chennai, Tamil Nadu, India

Corresponding author: Jenisha C, Email: [jenisha@saveetha.ac.in](mailto:jenisha@saveetha.ac.in)

The main objective of this paper is to present a detailed study on various recent innovations in haze removal techniques. The suspended particles in the atmosphere like mist, fog, and haze cause the captured picture to get degraded. Hence to get a clear image the dehazing technique is essential and the dehazing technique is also important since it is used for various applications like urban transportation, video analysis, visual surveillance, Image Processing, computer vision, outdoor photography, medical imaging for diagnostic purposes, object detection, object recognition, etc. In this paper, we have classified the existing dehazing techniques into Multiple and Single Image dehazing techniques and explained the significance of each method in detail. This paper also presents the outcomes of the DCP, CAP, MLP, DehazeNet, and PMS-Net dehazing methods by assessing the resultant dehazed image visually by qualitative analysis and by calculating the MSE, RMSE, PSNR, SSIM, BRISQUE, and FADE evaluation metrics by quantitative analysis. Thus, this paper helps the nurturing researchers who are doing their research work in this field, to acquire a wide knowledge about the various haze removal techniques.

**Keywords:** Dehazing Techniques, Haze Optics Model, Image Restoration, Analysis of Evaluation Metrics.

## 1 Introduction

The Haze is a slight obscuration of the lower atmosphere, typically caused by fine suspended particles in the air like dust, smoke, and other dehydrated elements that vague the clearness of the sky. The image taken beneath the hazy weather condition, causes only a certain reflected scene light to reach the camera and this occurs owing to the impacts of atmospheric absorption and scattering occurred by haze and in turn, this produces low contrast, reduction in scene clarity, the introduction of faded colors, loss of depth information, and decreases the pictorial quality [1]. The haze also affects the computer vision and image processing applications. Hence the dehazing technique is important in the field of various image understanding and computer vision applications. At present, there exists numerous dehazing techniques. In the past decades the dehazing techniques depends on the extra information like depth of the image, same image captured at different polarization, geographic 3D method, and images taken from diverse climatic conditions. But now, most of the existing dehazing techniques are realized based on the haze optical model [2,3]. The derivation of the haze optics model equation is clearly explained by DatNgoetal [4].

The hazy image is expressed in Equation (1) as

$$I(x)=J(x)t(x)+A(1-t(x)) \quad (1)$$

where,  $x$  is the pixel coordinate,  $I(x)$  is the hazy image,  $J(x)$  is the dehazed image,  $A$  is the global atmospheric light, and  $t(x)$  is the medium transmission coefficient.

The  $t(x)$  is expressed in Equation 2 as:

$$t(x)=e^{-\beta d(x)} \quad (2)$$

Where  $\beta$  is the scattering coefficient and  $d(x)$  is the scene depth. The goal of haze removal is to recover the scene  $J$ . The challenge is to estimate the  $A$  and  $t(x)$  from the single image  $I$  [4].

This is a review paper on different recent innovations in haze removal techniques where the algorithms utilized by different authors to generate haze-free images, their outcomes are presented. Section 2 explains the evaluation metrics of dehazed images. Section 3 explains the papers related to haze removal techniques. Section 4 presents the experimental outcomes in terms of qualitative and quantitative analysis of the various dehazing techniques. Finally, the paper concludes and reflects the thoughts on haze removal techniques.

## 2 Evaluation Metrics

This section gives a detailed description of the diverse evaluation metrics utilized by different authors in this paper for assessing their resultant dehazed images. In general, the resultant dehazed images are assessed visually by qualitative analysis and by calculating certain evaluation metrics by quantitative analysis. Some quantitative evaluation metrics have different notations since for the same evaluation metrics different authors in their paper use different notations and it is also mentioned below in Table1.

**Table 1.** Evaluation Metrics

<b>Quantitative Evaluation Metrics</b>	
<b>Notations</b>	<b>Descriptions</b>
PSNR	Peak Signal-to-Noise Ratio
SSIM	Structural Similarity
QSSIM	Average of SSIM
MSE	Mean Squared Error

FSIM	Feature Similarity
FSIMc	Extension of FSIM to color images
T/S / RT / T	Running Time / Time cost of dehazing process / Recovery Time
SSEQ	Spatial–Spectral Entropy-based Quality
BRISQUE/ $\alpha$ BR	Blind/Referenceless Image Spatial Quality Evaluator
NIQE/ $\alpha$ NIQ	Natural Image Quality Evaluator
$\Delta H$	Difference between Dehazed Image and its Original Image
$\alpha$ GCF	Global Contrast Factor
SD/ $\alpha$ S	Standard Deviation
$\alpha$ EI	Edge Intensity
$\alpha$ NAE	Normalized Absolute Error
$e / e_r$	the new apparent edge ratio
$\bar{r} / r$	normalize gradient of the visible edge
$\sigma / \varepsilon / \sigma_s / \Sigma$	The proportion of saturated white or black pixels
PCQI	Patch based Contrast Quality Index
Blur metric	Blur metric
BIQI	Blind Image Quality Indices
h	color retention degree
s	Edge Preserved Index EPI
$E_{avg}$	Average Absolute Error
IVM	Image Visibility Measurement
$C_{gain}$	Contrast gain
VCM	Visual Contrast Measure
CVD	Colour Variance Distance
IIE / IE / E / H	Image Information Entropy / Information Entropy / Entropy
CD	Color Difference
ISS	structure function of SSIM
CIEDE2000	CIE Color Difference Formula 2000 Version
WPSNR	Weighted Peak Signal-to-Noise Ratio
d	haze density
CR	Contrast Ratio
ESI	Edge Saved Index
RMSE	Root Mean Squared Error
RREE	Restoration Ratio of Effective Edges
UIQI / UQI	Universal Image Quality Index
VIF	Visual Information Fidelity
NIQMC	No-Reference Quality Metric
DIFF	DIFFerence between dehazed and ground truth
Q	measure combined effect of $e$ , $\bar{r}$ , and
UCIQE	Underwater Color Image Quality Evaluation
FADE	Fog Aware Density Evaluator
IC	Image Contrast
MAE	Mean Absolute Error
IL-NIQE	Integrated Local Natural Image Quality Evaluator
Ag	Mean gradient
Precision ratio	Precision ratio
Recall ratio	Recall ratio
CNR	Contrast-to-Noise Ratio
Saturation	Percentage of Saturated Pixels
user-selection	subjective user study

From the above quantitative evaluation metrics table, the higher values of PSNR, FSIM, FSIMc,  $\alpha$ GCF, SD,  $\alpha$ EI,  $e$ ,  $\bar{r}$ , PCQI, h, s,  $C_{gain}$ , IVM, VCM, CVD, IIE, ISS, WPSNR, CR, ESI, RREE, UIQI, VIF, Q, UCIQE, IC, Ag, precision ratio, recall ratio, CNR and user-selection metrics, and the lower values of MSE, SSEQ,

RT, BRISQUE, NIQE,  $\Delta H$ ,  $\alpha NA E$ ,  $\sigma$ , Blur metric, BIQI,  $E_{avg}$ , CD, CIEDE2000, d, RMSE, NIQMC, DIFF, FADE, MAE, IL-NIQE, and saturation metrics demonstrate the better performance of the resultant dehazed image. Furthermore, the higher and lower value of the SSIM metric depends on the reference image, i.e., if the clear haze-free image is taken as a reference image then the SSIM value must be higher to produce better performance and if the hazy image is taken as a reference image, then the SSIM value must be lower to provide better performance. Moreover, the robustness evaluation is carried out in the papers [5,6], where the authors evaluated the four-robustness evaluation called Airlight Robustness Evaluation (ARE), Coefficient Robustness Evaluation (CRE), Scale Robustness Evaluation (SRE), and Noise Robustness Evaluation (NRE), and proved the capability of their proposed method to remain same even for a small change in parameters.

### 3 Literature Review

At present in the haze removal research field, there are a wide variety of efficient theories and approaches have been proposed by researchers to address the problem of haze in the image. On examining, each researcher has utilized a different way to classify the existing dehazing techniques. The pictorial representation of dehazing methodology and classification is shown in Figure 1 below. In general, the dehazing techniques can be classified into Multiple Image Dehazing Techniques and Single Image Dehazing Techniques.

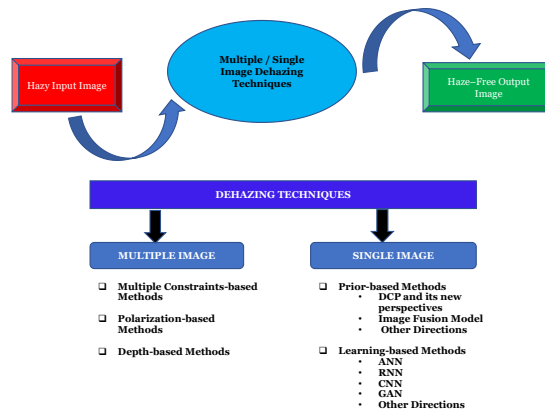


Fig. 1. Dehazing Techniques and Methodology

### **3.1 Multiple Image Dehazing Techniques**

The multiple image dehazing techniques deal with the multiple images and it can be further classified into three types they are Multiple Constraints-based methods, Polarization-based methods, and Depth-based methods.

#### **3.1.1 Multiple Constraints-based Methods**

Nayar and Narasimhan (1999) proposed a dichromatic atmospheric scattering model to examine the shading varieties in the scene under various climatic conditions. For a few vaporizers, in any case, scattering unequivocally relies upon the wavelength of occurrence light. Besides, scene recuperation utilizing the dichromatic model is vague for scene focuses whose tones match the shade of haze or dimness[7]. Hence during the year 2000, they introduced an overall chromatic structure for scene understanding under awful climate conditions and it is based on the prevailing dichromatic model. A few valuable constraints on scene shading changes due to various atmospheric conditions were inferred by the authors. Utilizing these constraints, the authors created simple algorithms to recuperate the three-dimensional structure and real nature of scenes, from pictures taken under bad climate conditions [8]. And again, during 2003 they put forward a physics-based method to reestablish the contrast of a scene from at least two pictures taken in the same awful climate conditions. Here this monochrome atmospheric scattering model depicts how homogeneous climatic conditions affect the scene intensities. The authors describe that this model is substantial in both the visible and near Infra-Red (IR) spectra, and for a wide scope of climate conditions like fog, cloudiness, mist, and different mist concentrates [3].

#### **3.1.2 Polarization-based Methods**

Yoav Y. Schechner et al. (2001, 2003) put forward polarization-based dehazing techniques. Initially, the image formation structure is designed on the fact by considering the partial polarization of atmospheric scattering in the presence of haze. After which by using this model not only produces the dehazed image but also yields details about the scene structure and the thickness and size dissemination of the atmospheric particles. The authors have also found that under rain the air light is partially polarized hence this proposed technique can be utilized. The authors conclude that for future work it can be stretched out to other dispersing media like underwater conditions or eventissues [9,10]. Sarit Shwartz et al. (2006) introduced a blind haze separation technique to recover the haze-free image. A critical advance in scene recuperation is the deduction of the airlight. Specifically, this can be accomplished by examining the polarization-filtered image. Nonetheless, the recuperation needs estimation of the airlight parameters. This paper infers a methodology for blindly recuperating the parameter required for isolating the airlight from the estimations, hence recuperating contrast, with neither client association nor presence of the sky in the outline. The proposed method has produced better results with real-world hazy images. Even though the proposed method has simplified the connections and conditions required for picture dehazing, the compensation for the lessening, is not blind, however requires some client communication. Further work is expected to set up a blind assessment. The authors conclude that this work can be extended to other dissipating modalities, like submerged photography[11]. Due to the high degree of polarization and the consequence of sunlight, the instant dehazing method wrongly represents the nearby objects as far away objects, hence to overcome this drawback the Mohamed Reda et al. (2017) introduced a polarization guided AutoRegressive (AR) model for depth recovery. Initially, to get dehazed image and estimated depth map, the instant dehazing method is applied on the two registered perpendicular polarized haze input images ( $I_0$  and  $I_{90}$ ) and here the registration of two polarized images is done by maximization of mutual information. After which the authors have constructed the datasets containing estimated depth

map and stroke vector component  $s_0$  and  $s_1$ , where stroke vector component is calculated from two perpendicular polarized images. Finally, by the proposed method the depth map is recovered by using  $I_{90}$  and  $s_1$ . Thus, the authors have proved that their recovered depth map by the proposed method outperforms than dark channel method and ADaptive color-guided AutoRegressive model (ADAR) model[12].

### **3.1.3 Depth-based Methods**

S. K. Nayar and S. G. Narasimhan (2003) introduced interactive (de) weathering of an image using physical models. This method provides a solution of dehazing a single image by not considering any particular weather or depth information. It works based on a physics-based model which is defined in earlier methods work. Here in this method, the three interactive algorithms are created which are used for eradicating as well as for adding weather into a single image. The merit of the proposed work is simple to use and be able to efficiently renovate clear day colors and also contrasts from bad climatic images. The authors have also presented pictorial outcomes of both eradicating as well as adding haze into an image [13]. Kopf et al.(2008) proposed a deep photo for perusing, enhancing, and maneuvering outdoor photos which work by joining them with previously prevailing georeferenced digital terrain and urban models. Here through utilizing a simple interactive registration process, the photograph is made to align with that model. Now, when the photo and the model have been registered, a bounty of data, like depth, texture, and GIS information, turns out to be quickly accessible by a deep photo. This data, thusly, empowers an assortment of activities, ranging from dehazing and relighting the photo, to novel view synthesis, and overlaying with geographic data. The author's outcomes show that increasing photos with effectively accessible 3D models of the world backups a wide variety of new ways to encounter and associate with our usual previews[14].

Although the above discussed multiple image dehazing techniques are easy to use and provided good results, it becomes difficult to obtain geometrical data and multiple pictures in real-world applications.

## **3.2 Single Image Dehazing Techniques**

At present, a lot of research work is proposed in single image dehazing techniques due to its strong priors and assumptions. We have classified single image dehazing techniques into three types they are prior-based methods, and learning-based methods.

### **3.2.1 Prior-based Methods**

#### **3.2.1.1 Dark Channel Prior (DCP) and its new perspectives**

R. T. Tan (2008) presented a single image dehazing technique. This technique depends on two fundamental perceptions: first, pictures with upgraded perceivability have more contrast than pictures tormented by terrible climate; second, airlight whose variety predominantly relies upon the distance of objects to the onlooker, will, in general, be smooth. Depending on these two perceptions, the authors constructed the cost function in the framework of Markov random fields, which can be proficiently enhanced by different procedures, like graph-cuts or belief propagation. The proposed method does have certain shortcomings like high computational time, halos at depth discontinuities, the outputs incline to have higher saturation values. Hence in the future work need to be done to eliminate the above limitations and to extend it to use for underwater images[15]. The Dark Channel Prior (DCP) dehazing method proposed by Heetal (2011) is a very simple method where the background working of this method, is based on the presence of the darkest pixel (low intensity) in one or more Red Green

Blue (RGB) color channels of outdoor haze-free images taken in a sky-free region. To estimate atmospheric light, at first, the top 0.1% brightest pixels in the dark channel are selected since these pixels are generally haze-opaque. Then amid these pixels, the input image which has the highest intensity pixels is chosen as the atmospheric light. Furthermore, the transmission map is correctly estimated by these dark pixels, and again to remove the presence of certain halo and block artifacts the estimated transmission map is further refined by the proposed soft matting. Finally, by the estimated atmospheric light and transmission map, the scene radiance is restored. It suffers from limitations like it is not suitable for the hazy images with the snowy ground or a white wall scene since the scene becomes integrally same as to the airlight and it also fails in certain risky conditions where the haze removal process itself becomes crucial because the haze becomes rarely visible [16]. Zhu et al. (2015) proposed a novel Color Attenuation Prior (CAP) model to remove haze from the single input hazy image. Initially, the linear model is constructed for the scene depth of the input hazy image. Then the linear model parameters can be easily learned by supervised learning by which the extension among the hazy image and its consequent depthmap is created successfully. Now the haze can be easily eliminated by the recuperated depth data. It suffers from limitations like under an inhomogeneous atmosphere environment the scattering coefficient of the atmospheric scattering model cannot be stated as constant [17]. Huang et al. (2014) put forward a novel Visibility Restoration (VR) dehazing method to remove haze from the images taken in real-world inclement weather conditions. Here to restore the haze-free image from the hazy image the proposed novel VR method contains three different modules are, Depth Estimation (DE) module, Color Analysis (CA) module, and VR module. All these three modules work one after the other to produce dehazed image. The effectiveness of the proposed method is checked by evaluating quantitative metrics [18]. Chen and Huang (2016) proposed Edge Collapse-Based dehazing technique for removing haze from the realworld and synthetic hazy images. Here the global atmospheric light is evaluated based on the Dark Channel Prior method. Then the authors have explained the image restoration of the proposed technique in three divisions they are haze density estimation, edge collapse repair, and image visibility recovery. For the quantitative assessment, the metrics calculated are MSE, PSNR, SSIM, and VIF. The authors showed better results both qualitatively and quantitatively while comparing the proposed technique with other dehazing techniques and also described the less computation time [19].

Wang et al (2018) put forward a three-variational model technique by combining Dark Channel Prior (DCP) and Total Variations (TV) for simultaneously removing noise and haze from the input hazy and noisy image. Initially, by DCP, the transmission map is related with depth is evaluated, and then based on this evaluation three variational models called Layered Total Variation (LTV) regulariser, Multichannel Total Variation (MTV) regulariser, and Colour Total Variation (CTV) regulariser are proposed for dehazing and denoising the color image. The authors have also introduced a new algorithm called the fast split Bregman algorithm which is quite different from already existing methods like the gradient descent method and Lagrangian multiplier method for improving the computational efficiency of the above proposed three models. The experimental work is done on a PC with Intel® Core™ CPU i5-4590, at 3.3GHz and 4GB memory using Matlab 2013a software. The authors concluded that the CTV model is effective and robust while comparing it with various other existing state-of-the-art methods [20]. The super pixel-based haze removal is proposed by Yang et al. (2018), for removing haze from the night time hazy image. Initially in this method, based on the relative smoothness of the nighttime hazy image, it is divided into a glow and glow-free nighttime hazy image. For image dehazing glow free night time hazy image is used and it is the same as that of day time hazy image except that, it has to change atmospheric light. The super pixel-based method is applied to the glow-free nighttime hazy image, to estimate the value of atmospheric light and dark channel of each pixel. This dark channel is decomposed into a transmission map by the Weighted Guided Image Filter (WGIF). The nighttime haze-free image is now recovered by using estimated atmospheric light and transmission map. The advantage of this method is that it conserved the local fine

details, and also it reduced the color distortion and halo artifacts. The drawback of this method is that it takes a much longer running time and it also quite complex. The authors concluded that for future research work, the problem to be addressed is to reduce the increasing noises in the sky region [21]. In most of the prevailing dehazing techniques, the haze-free image is improved using adjusting the contrast and saturation, but this adjustment causes the luminance to move away from its ideal value. Hence to overcome this shortcoming the Liu et al. (2019) proposed a configurable contrast enhancement model based on dark channel prior. The proposed model is designed by three modules they are transmission module, luminance module, and atmospheric light module. One of the merits of this proposed model is that it takes only 0.55 s of time to execute a one-megapixel of image. The authors evaluated the model with both subjective and objective assessments on the various Synthesized hazy image, natural scene hazy images, real- world hazy images. Thus, authors showed that their proposed model performs better than other methods in obtaining haze-free image even for images with high haze and also for images which have fair visibility visually. Therefore, the authors conclude that this work is much the same as atmospheric models hence it can be widened for image matting or alpha blending[22]. Berman et al. (2020) put forward a dehazing technique based on an approach novel non-local prior. This method is based on the statement that in the haze-free image, there will be a presence of few hundreds of different colors and these few hundreds of different colors become few hundreds of tight color clusters in RGB space but in the hazy image, these tight color clusters become a line in RGB space, which is named as haze-line. Based on these haze-lines, the proposed algorithm restores haze-free images by estimating the atmospheric light and transmission map. The merits of the proposed algorithm as compared with other dehazing methods are pixel-based approach rather than patch-based approach, doesn't need training and linear complexity. The experimental tests were done on various real-world images and the proposed algorithm results are compared with other dehazing methods by visually, evaluating quantitative metrics SSIM and CIEDE2000, and then robustness analysis. Even though the proposed algorithm works better than other dehazing techniques it fails to work for images with non-uniform lighting (i.e.) produces artifacts in the dehazed result [23]. Recently J. Jackson et al. (2020) presented a single image dehazing technique based on dark channel prior and Rayleigh scattering. Here the haze-free image is restored by solving the atmospheric scattering model (i.e.) by estimating the atmospheric light and transmission map. The authors proved that their presented method achieves better results on comparing with other dehazing methods both visually and also by examining the parameters  $e$ ,  $\bar{r}$ , and  $\sigma$ . The main advantage of this method is that the proposed method takes less computational time as compared with other dehazing methods hence this method works very fast. Even though the presented method has achieved good results; the authors have mentioned some of the drawbacks of this method. The drawbacks are in the dehazed image there exists a small percentage of artifacts and the transmission map needs extensive optimization. Thus, the authors conclude that the drawbacks can be considered for future research work [24].

### **3.2.1.2 Image Fusion Model**

Xuemei Wang et al. (2017) put forward a dehazing technique based on a physical imaging model. The authors proposed multiple priors for evaluating atmospheric light based on the new estimation of considering the probability, that a pixel is related to atmospheric light. The authors have also proposed a method for determining the transmission map (i.e.) initially a rough transmission map is evaluated by Laplace Pyramid (LP) fusion process and then it is filtered by a Total Variation (TV) model. The future work needs to be done to process the hazy image captured under inhomogeneous atmosphere and uneven incident light [25]. The local linear fusion dehazing method proposed by Yakun Gao et al. (2017) is developed based on the image fusion technique. In this method, the authors have given preference to enhance the haze-free image rather than accurately evaluating atmospheric light and transmission map. Hereby combining the depth information and subtracting the haze layer from the

RGB color channels of the hazy image, the first input image is obtained. The first input image is used to enhance the color saturation of the haze-free image. Then gamma correction is applied to the grey image of the input hazy image and after which by enhancing the details of the gamma-corrected image, the second input image is produced. Finally, the haze-free image is obtained after the fusion of the first and second input image by a local linear fusion model. The authors concluded that their method attained high contrast, clear textures, and fine details [26]. Guo et al. (2017) introduced a fusion-based estimation technique for dehazing hazy images and hazy videos in frames. Here in this technique, the authors have proposed a new method called Gaussian-based dark channel for estimating the atmospheric light. The authors have proposed Integral Contrast Limited Adaptive Histogram Equalization (ICLACHE), to get fine details from the whole image in a pixel-wise manner without color change even in light or dim area. Here in this technique, a new method called fusion weighting function is proposed to obtain transmission. To extend this method to utilize to remove haze in video frames, a method to remove the flickering effect in video frames is introduced [27]. The usage of the near-infrared image directly for haze removal will cause color distortion problem during the near-infrared fusion method hence to overcome this restriction, Son and Zhang (2018), introduced a new near-infrared fusion model which combines the conventional haze degradation model with the proposed new color and depth regularizations. The main goal of this model to eradicate color distortion and haze. The near-infrared image produces two types of images, one is the near-infrared gray image and the other is a visible color image. The proposed model results are quantitatively evaluated by calculating the metrics ISS and Color Difference (CD) [28].

### **3.2.1.3 Other Directions**

Ju et al. (2018) introduced a Gamma-correction-based Dehazing Model (GDM) which is designed based on relating Gamma Correction (GC) and atmospheric scattering model mathematically. The merits of this model are that the approximation of GDM into one-dimensional (1-D) function not only reduces the time required for haze removal but also it advances the renovation quality of the image and this happens by the search of only unidentified constant during the image restoration process. The drawback of this model is that GC capability is limited to some range in eliminating the haze from a single hazy image and it is also not easy to accomplish the best adjustment among the oversaturation of close-range regions and the complete dehazing of long-range regions. Therefore, these drawbacks need to be considered for future research work [29]. Kang and Kim (2018) presented a method called Conditional Random Fields (CRF) for obtaining dehazed images. The main advantage of this method over the several other existing methods is that; it can be used even in hazy images that have complex boundary regions for example forest pictures and it also eludes the filtering process. Here the calculation of atmospheric light is considered to be globally uniform and the transmission is estimated by CRF which contains unary factor and pairwise factor and it is updated iteratively by using the Tree-ReWeighted (TRW) message-passing algorithm. The quantitative analysis is done on real-world hazy images by calculating the parameter  $e$ ,  $r^-$ , and  $\sigma$  on synthesized hazy images the average QSSIM is obtained for the various scattering coefficient value [30]. The majority of the prevailing dehazing techniques restore the image based on the two-step strategy technique and due to this the transmission maps estimated may be incorrect and also the quality of scene radiance may lower. Hence to overcome this limitation the Wu et al. (2020) put forward a novel variational model that retrieves the transmission map and scene radiance together from a given single hazy and noisy image. The authors have used the same method as invented by He et al. for estimating atmospheric light. The authors introduce a transmission-aware nonlocal regularization to eradicate the enlargement of noise in the restored image. This proposed model suffers from two drawbacks one is, it does not work well for the hazy image with non-uniform air light and the second is, the segmentation cannot be efficiently updated. The authors suggest that the performance of dehazing and denoising can be increased by an

opting joint deep network[31]. Most of the existing model-based dehazing approaches have dehazing artifacts like color distortion and over enhancement around object boundaries which are caused by the inaccurate estimation of transmission from erroneous haze information, depth error in the sky line and it becomes exclusively true for the bright objects. Hence to eliminate the above limitations the Shin et al. (2020) proposed a novel optimization-based dehazing algorithm that joins the radiance-reflectance optimization and a structure-guided  $l_0$ -norm filter for removing haze from the image. Initially, the atmospheric light is evaluated by giving a minimum channel as an input to the quadtree search algorithm. Then the weak reflectance map is evaluated after which the transmission map is optimized based on the evaluated reflectance map. Finally, the dehazed image is obtained. The experimental work is done by utilizing the software MATLAB 2016b in the i7 Central Processing Unit (CPU) fortified with 16 GigaByte (GB) of RAM. Then, examine the synthetic images quantitatively by calculating the metrics PSNR, SSIM, CIED2000, and the real-world images are examined both visually and also by estimating the metrics CNR, entropy, NIQE, saturation, and the user-selection. Although it has obtained good results for synthetic and real-world hazy images however it fails for hazy images with multiple physical models like nighttime images and underwater images[32].

### **3.2.2 Learning-based Methods**

#### **3.2.2.1 Artificial Neural Network (ANN)**

Chen et al. (2018) presented a method Radial Basis Function (RBF) artificial neural network for restoring dehaze images from hazy images. This network uses an unsupervised learning approach and it consists of input, hidden, and output layers and it has a training and testing phase. During the training phase, the multi atmospheric veil model is used to form a hidden layer by unsupervised learning. During the testing phase the more visible edges are retained in the dehazed images and also the brightness of the dehazed images can be at tuned by the activation function of the hidden and output layer. The resultant dehazed images of this method yielded better results in terms of qualitative, quantitative, and performance metrics as compared with other methods. In the quantitative examination, this method produced weak stability since it has not yielded the lowest standard deviation. In the future work need to be done to improve the qualitative and quantitative results of this method[33]. Sebastian Salazar-Colores et al. (2018) examined that in the conventional DCP method the computation of transmission map of the input image requires two phases. The estimation of the transmission map and the refinement of the transmission map are the two processes. The main disadvantage of these strategies, however, is the trade-off between accurate restoration and time consumption. Hence to overcome this limitation, Sebastian Salazar-Colores et al. proposed a MultiLayer Perceptron (MLP) to compute the transmission map directly from the minimum channel and a contrast stretching technique. The authors proved that their proposed method performs better than the conventional DCP method in terms of accurate image restoration and time consumption[34].

#### **3.2.2.2 Recurrent Neural Network (RNN)**

Jiang et al. (2018) introduced a recognition algorithm based on recurrent neural networks for obtaining fog-free video images. This method initially, takes out the texture features of the image and all types of fog-associated color features using a sparse automatic coding machine. Then the recurrent neural network is used to obtain a mapping relationship between texture structure features and color features and scene deep map of fog images by the execution of sample training process. At last, by the scene deep map of foggy images, the fog-free images are obtained by atmospheric scattering model. The experimental tests were done on the forest and building vide of og images and also compared their experimental outcomes like running time, objective evaluation with other methods and proved better

results[35]. Recently the authors' Li et al. (2020) proposed a task-oriented network and multi-stage dehazing algorithm for image dehazing which over comes the problem of color distortion or artifacts. The motivation behind this work is the image formation of the hazing process based on the atmospheric scattering model. The input and output of this network is the hazy and clear image. The task-oriented network consists of an encoder and decoder network and a spatially variant recurrent neural network. The authors designed a loss function dual composition loss, content-based pixel-wise loss, and total variation constraint to set a limit to the proposed network. In this paper, the authors have done a broad analysis of the proposed network and loss function with various hazy datasets and also calculated the quantitative metrics PSNR and SSIM. Finally, the authors conclude that the proposed network and loss function has provided better results while comparing with other state-of-the-art methods [36].

### **3.2.2.3 Convolutional Neural Network (CNN)**

Cai et al. (2016) proposed a DehazeNet for the refurbishment of haze-free images. It is an end-to-end system that works based on a trainable Convolutional Neural Network (CNN) for obtaining a medium transmission map. Here the atmospheric light value is not considered a global constant rather it is erudite along with the medium transmission map in a combined network. The DehazeNet architecture performs four consecutive processes for assessing transmission maps, they are feature extraction, multi-scale mapping, local extremum, and nonlinear regression. The layers and nonlinear activations in DehazeNet are established in such a way to implement the above-mentioned four processes. This network accepts a hazy image as input and after the four consecutive processes, it produces a transmission map as output. After the estimation of the atmospheric light and medium transmissions map the haze-free image is restored. The training is done on a PC with Nvidia GeForce GTX 780 GPU and the dehazing framework is tested in the software MATLAB 2014 A. For evaluating the efficiency and performance of the network, the quantitative, qualitative, and robustness assessment is carried out in a proposed network. The PSNR, SSIM, MSE, and WPSNR are calculated for assessing quantitatively, CRE, ARE, SRE, and NRE are calculated for robustness evaluation. In the future work need to be done to estimate the atmospheric light based on learning through a deep neural network and haze-free image need to be optimized directly by the end-to-end mapping system without the evaluation of transmission map [6].

C. Li et al. (2018) proposed a cascaded Convolutional Neural Network (CNN) for obtaining dehazed images. This learning-based method consists of the shared hidden layer which is followed by two sub networks. Here the shared hidden layer extracts the common features for the consequent two sub networks. The outputs of the shared hidden layer are given as an input to the two sub networks which work together (i.e.) one for estimating transmission map and another for global atmospheric light. The transmission map estimation subnetwork is made by densely connected CNN while the global atmospheric subnetwork by light-weight CNN. After this, the medium transmission is again refined by a guided image filter to remove the blocking artifacts. In the end, after the evaluation of model parameters, the dehazed image is obtained by atmospheric scattering model inversion. Future work needs to be done to remove the amplification of noise and artifacts. In this work, the authors have not presented the diagrammatic representation of global atmospheric light estimation since they expressed it is hard to produce in figure format [1].

Zhang et al. (2018) introduced a method Light Dual-Task Neural Network (LDTNet) for obtaining haze-free images. In this, the transmission map estimation and haze-free image restoration are reproduced at a time. The haze-free image restoration is supported by the transmission map estimation which enhances dehazing and improves network generalization capability. This method yielded an average PSNR of 24.6156 and SSIM of 0.9517 which are relatively high as compared with the results of other dehazing techniques. The authors have also shown the proposed algorithm capability which remains unaffected by small changes in parameters by using four types of robustness evaluation ARE, CRE, SRE, and NRE. In further work, this

algorithm can be extended by conducting simultaneous dehazing and other tasks like high-level object detection, tracking, low-level super-resolution, and image restoration[5].

Wei-Ting Chen et al. (2019) noticed that the failure of the traditional DCP method in bright and white scenes is caused due to the fixed patch size. To overcome this limitation, Wei-Ting Chen et al. put forward an adaptive and automatic patch selection model called Patch Map Selection Network (PMS-Net) for removing haze from the single image. This network is built based on CNN and it is designed in such a way as to select the proper patch size from the defined patch map. The effectiveness of the presented method is verified and showed better results while analyzing and comparing with other dehazing techniques both visually and also by calculating the metrics PSNR, SSIM, MSE, and CIEDE2000[37]. Yeh et al. (2020) put forward a single image dehazing technique called a Multi-Scale deep Residual Learning (MSRL-DehazeNet) technique which is designed based on the CNN, and it is entrenched into a proposed image decomposition-guided framework. Initially in this method, the given input hazy image is decomposed into base and detail components. Furthermore, the final haze-free image is obtained by combining the dehazed base component image and improved detail component image. The proposed MSRL-DehazeNet experimental work is done on a PC which is outfitted with Intel® Core™ i7-8700k processor, 32 GB memory, and NVIDIA GeForce GTX 1080 GPU. For experimental tests, synthetic and real-world images are taken. Thus, the authors proved that their proposed MSRL-DehazeNet performs better than other dehazing techniques while comparing the qualitative as well as quantitative results PSNR and SSIM and also produced lower computational complexity[38]. Q. Yi et al. (2020) proposed a progressive back-traced dehazing network based on multi-resolution recurrent reconstruction for producing a haze-free image. The super-resolution and recurrent residual learning motivated the author to develop this network. The multi-scale convolutional module with irregular kernel shape is proposed to excerpt fine-grain local structures and also to conserve the textures in the hazy images while restoring the image. The multi-resolution residual fusion module is proposed for effective reuse of graded information and also to regularly restructure the intermediate haze-free images by confirming that at various resolutions the network has dehazed well. The experiments are done on GPU GTX 1080Ti by using PyTorch. The authors have also displayed their pictorial results and showed how the proposed network is better than the atmospheric scattering model and methods based on CNN [39].

### **3.2.2.4 Generative Adversarial Network (GAN)**

Pang et al. (2019) presented a Haze Removal Generative Adversarial Network (HRGAN) method. The HRGAN has a generator network and discriminate or network. The usage of the two networks is derived by their name itself (i.e), the generator network generates the dehazed images, and the discriminator network differentiates the generated dehazed images from original images [40]. Park et al. (2020) proposed a single image dehazing method called heterogeneous Generative Adversarial Networks (GAN) which consists of Cycle-consistent Generative Adversarial Networks (CycleGAN) and conditional Generative Adversarial Networks (cGAN). The architecture framework of the proposed network consists of two phases. In the first phase, the Cycle GAN is trained by an unpaired outdoor dataset and it contains two generators G<sub>J cyc</sub>, G<sub>I cyc</sub>, and two discriminators D<sub>J cyc</sub>, D<sub>I cyc</sub>. In the second phase, the cGAN is trained accordingly to estimate the transmission map and atmospheric light. Here in this proposed network, the CycleGAN is used for generating haze-clear images whereas the cGAN is used for maintaining the textural details. The experimental tests were done on both indoor synthetic hazy images and outdoor real-world hazy images. Furthermore, the proposed network is evaluated qualitatively by assess its visual appearance and then evaluated quantitatively by calculating the metrics PSNR, SSIM, BRISQUE, and NIQE. The proposed network performs better than other dehazing techniques on both synthetic and real-world images. Finally, the authors conclude that in the future the problem of production of the slightly darker image due to the overestimation of atmospheric

light needs to be addressed [41]. Most of the prevailing dehazing techniques take into account transmission map estimation and dehazing as two distinct works and also take up the atmospheric light as constant. Hence to overcome this, recently Zhang et al. (2020) proposed a new multi-task end-to-end CNN-based network that jointly learns to estimate transmission maps and does image dehazing. Initially, to obtain the joint estimation of transmission map from input hazy image and then dehazed image from transmission map, the consideration of constant atmospheric light is relaxed in the standard image degradation model. The proposed network consists of three sections they are transmission map estimation, hazy image feature extraction, and a dehazing network which is guided through transmission map and hazy image features. The experimental work of the proposed network is done using the Python platform. The authors have carried out two thorough ablation studies, one is to explain the efficiency of diverse sections in the transmission map estimation and the other is to explain the enhancements attained via diverse sections of dehazing images. Even though the proposed network is capable of simplifying the maximum number of outdoor scenes at finest, it produces saturation of certain regions of specific images, henceforth, in the future work needs to be done on this to fine simplification around outdoor images [42]. The already available learning-based and hand crafted prior-based dehazing algorithms fail to perform well during haze removal. Hence to overcome this limitation the Chen et al. (2020) introduced a method called Patch-Map Hybrid Learning DehazeNet (PMHLD) for removing haze from the single hazy image. The PMHLD combines the advantages of a patch map-based hybrid learning technique and a Bi-Attentive GAN approach. Here the hazy image is given as an input to the network and then atmospheric light and transmission map are estimated. The atmospheric light is estimated using the developed estimation network which calculates the atmospheric light correctly. To estimate the transmission map initially, a patch map is calculated through the introduced Bi-Attentive Patch Map Selection Network (BAPMS-Net). For quantitative analysis of synthetic images, the metrics calculated are MSE, PSNR, SSIM, and CIEDE2000, and the real-world images are analyzed visually. The authors proved that the proposed network performs better than other state-of-the-art methods in terms of analyzing both quantitatively as well as qualitatively. The proposed network has overwhelmed the problem of color distortion. One of the drawbacks of this proposed network is that the restored images undergo an over-exposed problem especially for the high-intensity areas and it happens when using the default maximum patch size 120. The authors say that this problem can be overcome by applying a patch size of an even larger upper bound but by doing this the time consumption will be increased. Hence in the future work need to be done to overwhelm the tradeoff which occurs between the overexposed problem and time consumption [43].

### **3.2.2.5 Other Directions**

Liu et al. (2019) introduced Learning Aggregated Transmission Propagation Networks for multipurpose applications like haze removal, under water image enhancement, and single image rain removal. Here they designed Data-and-Prior-Aggregated Transmission Network (DPATN), combines the advantages of prior-driven and data-driven network models but evades their shortcomings. The DPATN transmission propagation is established by combining priors and data into a deep residual architecture [44]. To obtain a haze-free image based on the atmospheric scattering model, an accurate estimate of transmission map and atmospheric light is essential. As examined, most of the existing CNN-based dehazing methods have introduced several dehazing methods by giving importance to accurate estimation of transmission map rather than accurate estimation of atmospheric light, but here in this proposed method the accurate estimation of atmospheric light also plays an essential part in dehazing the image. Hence to overcome these shortcomings, C. Wang et al. (2020) put forward an end-to-end dehazing network called Deep Residual Haze Network (DRHNet) for single image dehazing and deraining where instead of estimating the transmission and atmospheric light the residual difference between the clear and hazy image is produced straightly. In the future, the DRHNet can be widened for

other applications like video dehazing and diverse image restoration applications[45]. S. Tangsakul and S. Wongthanavas (2020) proposed a novel single image dehazing called Deep Cellular Automata learning (DeepCA) which associates the concept of deep learning and cellular automata method. Here the authors have divided the proposed method into two main divisions: the first division is a cellular automata deep feature extraction, where the authors except the hazy image light sourcefeatureusingrulesvectorinmulti- layer cellular automata and the second division is a decision stage. After that, from the haze density class, the haze preserved parameter ( $\omega$ ) and the ratio of global atmospheric light value ( $\rho$ ) are defined and these parameters bestow improved transmission map, maintains the natural look in the image, and then eliminate oversaturation and halo artifacts problembywhichbest-dehazedimagecanbeobtained. Although the DeepCA has achieved better performance, it works slower than other dehazing techniques, it inclines to increase the prevailing image artifacts for a certain image scene, and for the heavily hazy images it corruptsthebackgrounddetailsorcolorofcertainobjectsbynoise.Hencetheauthorsconcludethatinthefuture workneedstobecarriedouttoeliminatetheabove-mentioned drawbacks, need to evaluate the transmission map directly without the use of parameters, and then make the DeepCA work faster[46]. Santra et al. (2018) proposed a dehazing method based on Patch Quality Comparator, it is inspired by the idea of comparing twopatchesandtelling which patchhas a higher haze than to tell thehazelevelofthepatch. The metrics SSIM and CIEDE2000 are calculated to analyze the dehazed result quantitatively. The limitation of this proposed model is that the atmospheric light (i.e.) environmental illumination is evaluated based on the already existing dark channel prior model, due to this the authors observed that their result is not permanently correct. The authors agree that by correct evaluation of environmental illumination, the result would be better but the correct evaluation of environmental illumination is not considered important in dehazing technique [47].

## 4 Experimental Results and Datasets

The resultant haze-free images of the dehazing methods are assessed statistically by examining them qualitatively and quantitatively. As previously explained in evaluation metrics section, the qualitative evaluation is done visually and the quantitative evaluation is done by calculating certain evaluation metrics. This section discusses briefly the experimental datasets utilized, qualitative evaluation, and quantitativeevaluation.

### 4.1 Experimental Datasets

In this paper, we have performed thequalitativeandquantitativeevaluationonthefivepairs ofreal-world in door and outdoor hazy and haze-free images of I-HAZE [48] and O-Haze [49] datasets. The image size of 640X480 pixels is utilized for our experimental analysis. Table 3. describes the various dehazing methods and their corresponding experimental implementation platform. The experimental tests were done on a laptopIntel(R) Core(TM) i5-9300HF CPU @ 2.40GHz 2.40 GHz, 8 GB RAM,using the simulation software MATLAB R2020a andPyCharm Community 2021.2.

**Table 3.** Dehazing Techniques and its Implementation

Datasets	Dehazing Techniques	Implementation Platform
I-HAZE [48] and	DCP [16]	MATLAB
	CAP [17]	MATLAB
O-HAZE [49]	MLP [34]	MATLAB
	DehazeNet [6]	MATLAB
	PMS-Net [37]	PyCharm

## 4.2 Qualitative Evaluation

We qualitatively compare the DCP, CAP, MLP, DehazeNet, PMS-Net, and PMHLD dehazing methods on five real-world indoor and outdoor hazy images. Figure 2 and Figure 3 represent the qualitative comparison of the various dehazing techniques.

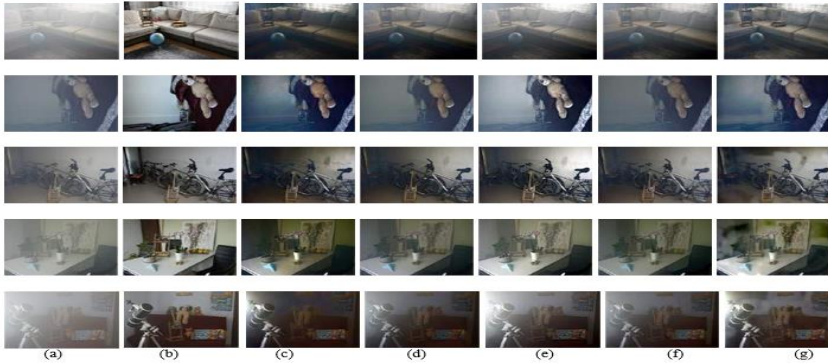


**Fig. 2.** Qualitative Comparison of various dehazing methods on a five real world indoor hazy images. (a) Hazy Image, (b) Ground Truth Image, (c) Results of DCP [16], (d) Results of CAP [17], (e) Results of MLP [34], (f) Results of DehazeNet [6], (g) Results of PMS-Net [37].



**Fig. 3.** Qualitative Comparison of various dehazing methods on a five real world outdoor hazy images. (a) Hazy Image, (b) Ground Truth Image, (c) Results of DCP [16], (d) Results of CAP [17], (e) Results of MLP [34], (f) Results of DehazeNet [6], (g) Results of PMS-Net [37].

## 4.3 Quantitative Evaluation

To avoid the inherent bias of qualitative comparisons and to quantitatively analyze the dehazed images properly, we compute the MSE, RMSE, PSNR, SSIM, BRISQUE, and FADE metrics. The higher values of PSNR, SSIM, and the lower values of MSE, RMSE, BRISQUE, FADE represent the better performance of the resultant dehazed images. The higher SSIM indicates a stronger structural similarity between the dehazed output and the ground truth image. Table 4 and 5 summarize the quantitative evaluation of the dehazed results in Figure 2 and Figure 3 using MSE, RMSE, PSNR, SSIM, BRISQUE,

andFADEWealsodeterminedtheaverage,median,andStandard Deviation (SD) of these metrics over the set of images to make measuring the success of different approaches easier. For PSNR and SSIM metrics the higher values of their corresponding average and median represent the better performance of the resultant dehazed images. For the MSE, RMSE, BRISQUE, and FADE metrics the lowervalueoftheircorrespondingaverageandmedianrepresents thebetterperformanceoftheresultantdehazed images. A smaller SD implies that each test image's value is close to the average evaluate for all test images, where as a greater SD shows tha teach test image's value is spread awayfromitsaveragevalue.Fortheconvenienceofthe reader, we also highlighted the better performance of each metric in the boldfont.

**Table 4.** Quantitative Comparisons of Dehazed Results in Figure 2 using MSE, RMSE, PSNR, SSIM, BRISQUE, and FADE.

Image Type	Metrics	DCP [16]	CAP [17]	MLP [34]	DehazeNet [6]	PMS-Net [37]
Five Indoor Images	MSE	0.0652	0.0417	0.0263	0.0314	0.0284
		0.0427	0.0388	0.0154	0.0446	0.0322
		0.0327	0.0162	0.0134	0.0111	0.0139
		0.0622	0.0337	0.0163	0.0422	0.0296
	MSE Average	0.0348	0.0230	0.0293	0.0186	0.0169
		0.04752	0.03068	<b>0.02014</b>	0.02958	0.0242
	MSE Median	0.0427	0.0337	<b>0.0163</b>	0.0314	0.0284
	MSE SD	0.01527	0.010784	<b>0.00715</b>	0.01458	0.008219
		0.2553	0.2043	0.1624	0.1772	0.1688
	RMSE	0.2067	0.1971	0.1244	0.2114	0.1796
		0.1809	0.1273	0.1160	0.1055	0.1182
		0.2494	0.1837	0.1278	0.2055	0.1722
		0.1867	0.1518	0.17131	0.1366	0.1301
	RMSE Average	0.2158	0.17284	<b>0.140382</b>	0.16724	0.15378
		RMSE Median	0.2067	0.1837	<b>0.1278</b>	0.1772
	RMSE SD	0.034774	0.032453	<b>0.024746</b>	0.045453	0.027651
		11.8574	13.7906	15.7863	15.0277	15.4523
	PSNR(dB)	13.6925	13.6486	18.1002	13.0428	14.4922
		14.8508	17.8985	18.7080	19.5317	18.5412
		12.0606	14.7177	17.8681	13.7402	15.2786
		14.5741	16.3710	15.3238	17.2864	17.7095
	PSNR Average	13.40708	15.28528	<b>17.15728</b>	15.72576	16.29476
	PSNR Median	13.6925	14.7177	<b>17.8681</b>	15.0277	15.4523
	PSNR SD	<b>1.391244</b>	1.819522	1.503357	2.671553	1.734901
	SSIM	0.4808	0.4913	0.5480	0.5210	0.6308
		0.7134	0.6978	0.7724	0.6855	0.7570
		0.7020	0.7680	0.8144	0.8199	0.8333
		0.6676	0.7284	0.7826	0.7139	0.7785
	SSIM Average	0.7497	0.7743	0.7915	0.7968	0.8592
		0.6627	0.69196	0.74178	0.70742	<b>0.77176</b>
SSIM Median	0.702	0.7284	0.7826	0.7139	0.7785	
SSIM SD	0.105825	0.116392	0.109431	0.118232	<b>0.088834</b>	
	12.5311	10.7551	8.6304	9.7585	1.3102	
BRISQUE	17.9596	20.1483	14.7792	26.4669	11.6388	
	7.3895	6.0492	10.0588	4.2537	-2.5949	
	15.5858	19.1577	10.6384	19.6109	4.2719	

		29.2236	25.0580	15.2247	25.4257	10.6580
	<b>BRISQUE</b>	16.53792	16.23366	11.8663	17.10314	5.0568
	<b>Average</b>					
	<b>BRISQUE</b>	15.5858	19.1577	10.6384	19.6109	<b>4.2719</b>
	<b>Median</b>					
	<b>BRISQUE SD</b>	8.117918	7.672699	<b>2.958449</b>	9.776064	6.080661
		1.0414	0.8753	1.2342	1.1799	0.8268
	<b>FADE</b>	0.5848	1.8483	0.7791	2.0991	0.6667
		0.6686	0.8971	0.5282	0.9626	0.6696
		0.8835	1.5571	1.1810	1.3101	0.7684
		1.1691	1.2879	1.1543	1.3726	0.8266
	<b>FADE Average</b>	0.86948	1.29314	0.97536	1.38486	0.75162
	<b>FADE Median</b>	0.8835	1.2879	1.1543	1.3101	0.7684
	<b>FADE SD</b>	0.245418	0.421112	0.30813	0.429008	<b>0.079835</b>

**Table 5.** Quantitative Comparisons of Dehazed Results in Figure 3 using MSE, RMSE, PSNR, SSIM, BRISQUE, and FADE.

Image Type	Metrics	DCP [16]	CAP [17]	MLP [34]	DehazeNet [6]	PMS-Net [37]
Five Outdoor Images	<b>MSE</b>	0.0280	0.0412	0.0633	0.0538	0.03152
		0.0301	0.0259	0.0224	0.0230	0.01609
		0.0110	0.0174	0.0161	0.0129	0.0071
		0.0091	0.0151	0.0310	0.0195	0.0214
		0.0228	0.0274	0.0257	0.0421	0.0172
	<b>MSE Average</b>	0.0202	0.0254	0.0317	0.03026	<b>0.018662</b>
	<b>MSE Median</b>	0.0228	0.0259	0.0257	0.023	<b>0.0172</b>
	<b>MSE SD</b>	0.009663	0.010295	0.018472	0.01706	<b>0.008878</b>
	<b>RMSE</b>	0.1673	0.2031	0.2516	0.2319	0.1775
		0.1734	0.1611	0.1497	0.1518	0.1268
		0.1053	0.1321	0.1270	0.1138	0.0843
		0.0957	0.1231	0.1760	0.1397	0.1463
		0.1511	0.1657	0.1605	0.2053	0.1311
	<b>RMSE Average</b>	0.13856	0.15702	0.17296	0.1685	<b>0.1332</b>
	<b>RMSE Median</b>	0.1511	0.1611	0.1605	0.1518	<b>0.1311</b>
	<b>RMSE SD</b>	0.035848	0.031571	0.04744	0.048668	<b>0.033803</b>
	<b>PSNR(dB)</b>	15.5269	13.8426	11.9839	12.6903	15.0133
		15.2147	15.8559	16.4937	16.3703	17.9319
		19.5470	17.5771	17.9205	18.7727	21.4809
		20.3767	18.1895	15.0857	16.9225	16.6903
		16.4141	15.0826	15.8870	13.2249	17.1169
	<b>PSNR Average</b>	17.41588	16.10954	15.47416	15.59614	<b>17.64666</b>
	<b>PSNR Median</b>	16.4141	15.8559	15.887	16.3703	<b>17.1169</b>
	<b>PSNR SD</b>	2.383544	<b>1.784511</b>	2.209485	2.574673	2.393356
<b>SSIM</b>	0.5286	0.4110	0.5060	0.4266	0.6523	
	0.6003	0.5671	0.6356	0.5912	0.7446	
	0.7799	0.6846	0.7691	0.7210	0.8497	
	0.7571	0.6378	0.7408	0.6499	0.8100	
	0.5803	0.5019	0.6934	0.4618	0.6775	
<b>SSIM Average</b>	0.64924	0.56048	0.66898	0.5701	<b>0.74682</b>	
<b>SSIM Median</b>	0.6003	0.5671	0.6934	0.5912	<b>0.7446</b>	
<b>SSIM SD</b>	0.112258	0.108632	0.10423	0.124404	<b>0.084143</b>	

	18.4275	19.5707	19.6665	15.1301	24.1156
<b>BRISQUE</b>	22.5945	26.7719	23.8213	26.4430	23.6292
	34.9240	23.1309	37.7190	21.3819	33.5670
	21.7219	20.4038	33.7750	20.1382	24.7830
	16.7210	16.0994	25.8612	15.3549	14.1504
<b>BRISQUE Average</b>	22.87778	21.19534	28.1686	<b>19.68962</b>	24.04904
<b>BRISQUE Median</b>	21.7219	20.4038	25.8612	<b>20.1382</b>	24.1156
<b>BRISQUE SD</b>	7.145604	<b>4.002468</b>	7.401869	4.697132	6.879208
	0.3797	0.4149	0.5115	0.6572	0.3827
	0.3502	0.5505	0.4185	0.7761	0.4066
<b>FADE</b>	0.2037	0.3256	0.2813	0.4180	0.2132
	0.1904	0.3517	0.1891	0.4013	0.2542
	0.3452	0.7433	0.2567	1.1157	0.3941
<b>FADE Average</b>	<b>0.29384</b>	0.4772	0.33142	0.67366	0.33016
<b>FADE Median</b>	0.3452	0.4149	<b>0.2813</b>	0.6572	0.3827
<b>FADE SD</b>	<b>0.089458</b>	0.172334	0.13073	0.293984	0.08964

## 5 Conclusion

Here, a detailed review of diverse single image haze removal techniques proposed by different authors was presented. The presence of haze in the atmosphere causes the captured picture to get degraded hence to remove haze from the image, dehazing techniques are introduced. The dehazing techniques also play a vital role in several real-time applications like urban transportation, video analysis, visual surveillance, Image Processing, computer vision, outdoor photography, object detection, object recognition, medical imaging for diagnostic purposes, etc. We have done a qualitative and quantitative experimental test on the dehazing techniques like DCP, CAP, DehazeNet, MLP, and PMS-Net by using I-HAZE and O-HAZE datasets. From this paper, we can see how dehazing techniques have emerged up well since different authors work in this field to propose several novel innovative dehazing techniques. Each dehazing technique discussed in this paper has its uniqueness. Some of the dehazing techniques discussed above do suffer from their shortcomings hence those methods need further improvement in the future. Most of the dehazing techniques mentioned above obtain a haze-free image by estimating atmospheric light and transmission maps. Further research work needs to be carried out in obtaining simultaneous dehazing and also to utilize it for other applications like high-level object detection, tracking, low-level super-resolution, and image restoration. Thus, we conclude the new research contribution and the innovative thoughts in this research field will keep evolving in the future.

## References

- [1] Chongyi Li, et al. (2018). A Cascaded Convolutional Neural Network for Single Image Dehazing. *IEEE Trans Med Imaging*, 6:24877-24887.
- [2] McCartney EJ. (1976). *Optics of the Atmosphere: Scattering by Molecules and Particles*. New York, NY, USA: Wiley.
- [3] Shree K Nayar, and Srinivasa G Narasimhan. (2003). Contrast restoration of weather degraded images. *IEEE Trans Pattern Anal Mach Intell*, 25(6):713-724.
- [4] Dat Ngo, Seungmin Lee, Tri Minh Ngo, et al. (2021). Visibility Restoration: A Systematic Review and Meta-Analysis. *Sensors*, 21, 2625:1-41.

- [5] Yu Zhang, Xinchao Wang, Xiaojun Bi, et al. (2018). A Light Dual-Task Neural Network for Haze Removal. *IEEE Signal Process Lett*, 25(8):1231-1235.
- [6] Bolun Cai, Xiangmin Xu, Kui Jia, et al. (2016). DehazeNet: An End-to-End System for Single Image Haze Removal. *IEEE Trans Image Process*, 25(11):5187-5198.
- [7] Shree K Nayar, and Srinivasa G Narasimhan. (1999). Vision in bad weather. in *Proceedings of the Seventh IEEE International Conference on Computer Vision*; 1999 Sept 20-27; Kerkyra, Greece, 820–827.
- [8] Srinivasa G Narasimhan, and Shree K Nayar. (2000). Chromatic frame work for vision in bad weather. in *Proceedings of the IEEE Conference on Computer Vision and Pattern Recognition*; 2000 June 15-15; Hilton Head, SC, USA, 598–605.
- [9] Yoav Y Schechner, Srinivasa G Narasimhan, and Shree K Nayar. (2001). Instant dehazing of images using polarization. in *Proceedings of the IEEE Computer Society Conference on Computer Vision and Pattern Recognition*, 2001 Dec 8-14; Kauai, HI, USA, 325– 332.
- [10] Yoav Y Schechner, Srinivasa G Narasimhan, and Shree K. Nayar. (2003). Polarization-based vision through a haze. *Appl Optics*, 42(3):511–525.
- [11] Sarit Shwartz, Einav Namer, and Yoav Y Schechner. (2006). Blind haze separation. in *Proceedings of the 2006 IEEE Computer Society Conference on Computer Vision and Pattern Recognition*; 2006 June 17-22; New York, NY, USA, 1984–1991.
- [12] Mohamed Reda, Yongqiang Zhao, and Jonathan Cheung-Wai Chan. (2017). Polarization Guided Autoregressive Model for Depth Recovery. *IEEE Photonics J*, 9(3): 6803016-6803016.
- [13] Srinivasa G Narasimhan, and Shree K Nayar. (2003). Interactive (de) weathering of an image using physical models. in *Proceedings of the ICCV '03 Workshop on Color and Photometric Methods in Computer Vision*; 2003 Oct, 6:1–4.
- [14] Johannes Kopf, Boris Neubert, Billy Chen et al. (2008). Deep photo: Model-based photograph enhancement and viewing. *ACM Trans Graph*, 27(5):116-1–116-10.
- [15] RT Tan. (2008). Visibility in bad weather from a single image. in *Proceedings of the 2008 IEEE Conference on Computer Vision and Pattern Recognition*; 2008 June 23-28; Anchorage, AK, USA, 1–8.
- [16] Kaiming He, Jian Sun, and Xiaoou Tang. (2011). Single Image Haze Removal Using Dark Channel Prior. *IEEE Trans Pattern Anal Mach Intell*, 33(12):2341-2353.
- [17] Qingsong Zhu, Jiaming Mai, and Ling Shao. (2015). A fast single image haze removal algorithm using color attenuation prior. *IEEE Trans Image Process*, 24(11):3522–3533.
- [18] Shih-Chia Huang, Bo-Hao Chen, and Wei-Jheng Wang. (2014). Visibility Restoration of Single Hazy Images Captured in Real-World Weather Conditions. *IEEE Trans Circuits Syst Video Technol*, 24(10):1814-1824.
- [19] Bo-Hao Chen, and Shih-Chia Huang. (2016). Edge Collapse-Based Dehazing Algorithm for Visibility Restoration in Real Scenes. *Journal of Display Technology*, 12(9):964-970.
- [20] Zhi Wang, Guojia Hou, Zhenkuan Pan, et al. (2018). Single image dehazing and denoising combining dark channel prior and variational models. *IET Comput Vis*, 12(4):393-402.
- [21] Minmin Yang, Jianchang Liu, and Zhengguo Li. (2018). Superpixel-Based Single Nighttime Image Haze Removal. *IEEE Trans Multimedia*, 20(11):3008-3018.
- [22] Ping-Juei Liu, Shi-Jinn Horng, Jzau-Sheng Lin, et al. (2019). Contrast in Haze Removal: Configurable Contrast Enhancement Model Based on Dark Channel Prior. *IEEE Trans Image Process*, 28(5):2212-2227.
- [23] Dana Berman, Tali Treibitz, and Shai Avidan. (2020). Single Image Dehazing Using Haze-Lines. *IEEE Trans Pattern Anal Mach Intell*, 43(3):720-734.
- [24] Jehoiada Jackson, et al. (2020). A Fast Single-Image Dehazing Algorithm Based on Dark Channel Prior and Rayleigh Scattering. *IEEE Access*, 8:73330-73339.
- [25] Xuemei Wang, Mingye Ju, and Dengyin Zhang. (2017). Image haze removal via multiscale fusion and total variation. *J Sys Eng Electron*, 28(3): 597–605.
- [26] Yakun Gao, Haiyan Chen, Haibin Li, et al. (2018). Single image dehazing using local linear fusion. *IET Image Process*, 12(5): 637– 643.
- [27] Jing-Ming Guo, Jin-yu Syue, Vincent R Radzicki, et al. (2017). An Efficient Fusion-Based Defogging. *IEEE Trans Image Process*, 26(9):4217-4228.
- [28] Chang-Hwan Son, and Xiao-Ping Zhang. (2018). Near-Infrared Fusion via Color Regularization for Haze and Color Distortion Removals. *IEEE Trans Circuits Syst Video Technol*, 28(11):3111-3126.
- [29] Mingye Ju, Can Ding, Dengyin Zhang, et al. (2018). Gamma-Correction-Based Visibility Restoration for Single Hazy Images. *IEEE Signal Process Lett*, 25(7):1084-1088.

- [30] Chunghun Kang, and Gyeonghwan Kim. (2018). Single Image Haze Removal Method Using Conditional Random Fields. *IEEE Signal Process Lett*, 25(6):818-822.
- [31] Qingbo Wu, Jingang Zhang, Wenqi Ren, et al. (2020). Accurate Transmission Estimation for Removing Haze and Noise From a Single Image. *IEEE Trans Image Process*, 29:2583-2597.
- [32] Joongchol Shin, et al. (2020). Radiance-Reflectance Combined Optimization and Structure-Guided L<sub>0</sub>-Norm for Single Image Dehazing. *IEEE Trans Multimedia*, 22(1):30-44.
- [33] Bo-Hao Chen, Shih-Chia Huang, Chian-Ying Li, et al. (2018). Haze Removal Using Radial Basis Function Networks for Visibility Restoration Applications. *IEEE Trans Neural Netw Learn Sys*, 29(8):3828-3838.
- [34] Sebastian Salazar-Colores, Ivan Cruz-Aceves, and Juan-Manuel Ramos-Arreguin. (2018). Single image dehazing using a multilayer perceptron. *J Electron Eng*, 27(4):043022.
- [35] Xiaoping Jiang, Jing Sun, Chenghua Li, et al. (2018). Video Image Defogging Recognition Based on Recurrent Neural Network. *IEEE Trans Industr Inform*, 14(7):3281-3288.
- [36] Runde Li, Jinshan Pan, Min He, et al. (2020). Task-Oriented Network for Image Dehazing. *IEEE Trans Image Process*, 29: 6523- 6534.
- [37] Wei-Ting Chen, Jian-Jiun Ding, Sy-Yen Kuo. (2019). PMS-Net: Robust Haze Removal Based on Patch Map for Single Images. In *Proceedings of the IEEE/CVF Conference on Computer Vision and Pattern Recognition (CVPR)*; 2019 June 15-20; Long Beach, CA, USA, 11681-11689.
- [38] Chia-Hung Yeh, Chih-Hsiang Huang, and Li-Wei Kang. (2020). Multi-Scale Deep Residual Learning-Based Single Image Haze Removal via Image Decomposition. *IEEE Trans Image Process*, 29:3153-316.
- [39] Qiaosi Yi, Alwen Jiang, Juncheng Li, et al. (2020). Progressive Back-Traced Dehazing Network Based on Multi-Resolution Recurrent Reconstruction. *IEEE Access*, 8:54514-54521.
- [40] Yanwei Pang, and Jin Xie, Xuelong Li. (2019). Visual Haze Removal by a Unified Generative Adversarial Network. *IEEE Trans Circuits Syst Video Technol*, 29(11):3211-3221.
- [41] Jaihyun Park, David K Han, and Hanseok Ko. (2020). Fusion of Heterogeneous Adversarial Networks for Single Image Dehazing. *IEEE Trans Image Processing*, 29: 4721-4732.
- [42] He Zhang, Vishwanath Sindagi, Vishal M Patel. (2020). Joint Transmission Map Estimation and Dehazing Using Deep Networks. *IEEE Trans Circuits Syst Video Technol*, 30(7):1975-1986.
- [43] Wei-Ting Chen, Hao-Yu Fang, Jian-Jiun Ding, et al. (2020). PMHLD: Patch Map-Based Hybrid Learning DehazeNet for Single Image Haze Removal. *IEEE Trans Image Process*, 29:6773-6788.
- [44] Risheng Liu, Xin Fan, Minjun Hou, et al. (2019). Learning Aggregated Transmission Propagation Networks for Haze Removal and Beyond. *IEEE Trans Neural Netw Learn Syst*, 30(10): 2973 -2986.
- [45] Chuansheng Wang, et al. (2020). Deep Residual Haze Network for Image Dehazing and Deraining. *IEEE Access*, 8: 9488- 9500.
- [46] Surasak Tangsakul, and Sartra Wongthanavasu. (2020). Single Image Haze Removal Using Deep Cellular Automata Learning. *IEEE Access*, 8: 103181-103199.
- [47] Sanchayan Santra, Ranjan Mondal, and Bhabatosh Chanda. (2018). Learning a Patch Quality Comparator for Single Image Dehazing. *IEEE Trans Image Process*, 27(9):4598-4607.
- [48] Cosmin Ancuti, Codruta O Ancuti, Radu Timofte, et al. (2018). I-HAZE: A dehazing benchmark with real hazy and haze-free indoor images. In *Advanced Concepts for Intelligent Vision Systems*; Blanc-Talon J, Helbert D, Philips W, Popescu D, Scheunders P, Eds; Springer International Publishing: Cham, Switzerland, 620-631.
- [49] Codruta O Ancuti, et al. (2018). O-HAZE: A Dehazing Benchmark with Real Hazy and Haze-Free Outdoor Images. In *Proceedings of the IEEE/CVF Conference on Computer Vision and Pattern Recognition Workshops (CVPRW)*; 2018 June 18-22; Salt Lake City, UT, USA, 867-8678.